

UC Irvine

UC Irvine Previously Published Works

Title

Cartilage Reshaping

Permalink

<https://escholarship.org/uc/item/2x56r4ht>

ISBN

978-3-030-29603-2

Authors

Gu, Jeffrey T
Wong, Brian JF

Publication Date

2020

DOI

10.1007/978-3-030-29604-9_13

Copyright Information

This work is made available under the terms of a Creative Commons Attribution License, available at <https://creativecommons.org/licenses/by/4.0/>

Peer reviewed



Cartilage Reshaping

13

Jeffrey T. Gu and Brian J. F. Wong

Contents

13.1	Introduction	154
13.2	Basic Science of Cartilage Reshaping	154
13.2.1	Laser Shaping of Cartilage	154
13.2.2	Ex Vivo Cartilage Reshaping	156
13.2.3	Cartilage Properties	157
13.2.4	Control Systems in Laser Cartilage Reshaping	162
13.3	Clinical Applications	162
13.3.1	In Vivo LCR	162
13.3.2	LCR of the Airway	164
13.3.3	LCR of Septal Cartilage	165
13.3.4	LCR of Auricular Cartilage	166
13.4	Conclusions	171
	References	171

Abstract

In this chapter, we introduce the working theory of cartilage reshaping and highlight landmark papers in the development and refinement of this technique. We discuss the tissue and mechanical properties of cartilage and define how optical techniques may be utilized to manipulate these properties. The goal of cartilage reshaping is to ultimately reduce the need for more invasive traditional approaches with

scalpel and suture, in favor of much less invasive techniques. Therefore, we discuss the challenges associated with its development and delineate its translation toward clinical applications.

Keywords

Cartilage reshaping · Optical techniques
Airway reshaping · Rhinoplasty · Otoplasty

J. T. Gu · B. J. F. Wong (✉)
Department of Otolaryngology-Head & Neck
Surgery, UC Irvine School of Medicine,
Irvine, CA, USA
e-mail: jtgu@uci.edu; bjwong@uci.edu

13.1 Introduction

Classical approaches to altering the shape of cartilage in the head, neck, and upper airway have focused on creating incisions in the cartilage to weaken it focally or using sutures to balance the forces which resist sustained deformation. Surgery as a whole is steeped in the use of these conventional approaches which require gaining access to individual cartilage specimens through incisions within the nose or neck.

Cartilage itself is a complex tissue which is triphasic in structure, having its mechanical state determined by the interplay of viscoelastic, hydrodynamic, and electrostatic forces. This specific behavior is well beyond the scope of this discussion here but has been examined in detail by Mow and Lai, among others [1–4]. Importantly, cartilage may be thought of as a charged polymer hydrogel, and if one examines cartilage from the vantage of a materials scientist, one can think of alternate ways of creating shape change, without the need potentially for either destructive techniques involving scalpels or techniques involving sutures. Early in the 1950s, Lewis Thomas, in fact, had examined the potential use of enzymes to locally disrupt the bonds between the glycosaminoglycans in the cartilage of rabbit ears and was able to demonstrate transient changes in tissue geometry [5–9]. While promising, the effect was noted to be completely reversible, which negated any further exploration of this approach toward clinical implementation.

In contemporary times, Emil Sobol of the Russian Academy of Sciences in Troitsk, while on sabbatical in Crete, had the opportunity to work with Emmanuel Helidonis, who is an otolaryngologist. Helidonis had an extensive medical laser facility, and Sobol spent his time identifying areas where advanced laser technology might optimize surgery. As an alternative to morselization, Sobol proposed that cartilage could be heated and then undergo a phase transformation that would lead to an alteration of shape. In this implementation, cartilage which is itself curved or misshapen is first mechanically deformed, and then laser energy is directed at areas where internal stress is concentrated. Focally within these

regions of interest, temperature elevation leads to a local alteration in tissue mechanical properties and an acceleration of stress relaxation.

The net effect is shape change, which in this case early on was focused on changing the shape of the nasal septal cartilage. Regardless, the use of photothermal techniques to reshape cartilage is still investigational, though much basic research has focused on this application. The use of lasers to reshape cartilage has been studied in great detail, though the precise mechanism still remains elusive. The hope and goal of this technique is that traditional cut-and-suture approaches to altering cartilage shape could be replaced by methods which are minimally invasive, potentially transcutaneous, or delivered via fiber optics and small-bore needles.

Likewise, in parallel with research performed in laser reshaping, other techniques that alter the shape of facial cartilages have been developed. These include the application of radiofrequency energy as well as the creation of in situ redox reactions in the tissue. All of these approaches do share in common a fundamental difference from classic surgical technique in that these view cartilage as a plastic material.

The remainder of this chapter reviews the basic science behind facial cartilage reshaping using laser and related technologies and provides a comprehensive review of the literature.

13.2 Basic Science of Cartilage Reshaping

13.2.1 Laser Shaping of Cartilage

In living organisms, cartilage serves to support and fasten soft tissues and to absorb shock for skeletal bones. Cartilage is a dense connective tissue composed of 65–80% of water containing a small proportion of chondrocytes within an extracellular matrix (ECM). The ECM is a hydrated gel containing proteoglycans (5–15%) and collagen fibers (20–25%). The proteoglycan matrix possesses negatively charged ion groups (SO_3^- and COO^- moieties). Therefore, cartilage can be thought of as a charged hydrogel where

free space is filled with water in either partially bound or free states. Polarized water molecules bind weakly to the negatively charged groups attached to both proteoglycan and collagen molecules. Free water within the cartilage matrix contains dissolved minerals such as Na^+ and Ca^{2+} ions, which are attracted to the negatively charged components of proteoglycan molecules (Fig. 13.1). These ions are therefore trapped in the matrix when free water is forced out of it during deformation or evaporation. A gradient in distribution of negatively charged groups in the tissue accounts for the intramolecular internal stresses of the tissue. Since the ECM is nonvascular, maintenance of its mechanical structure and nutrition for chondrocytes depends on the diffusion of fluids [11]. The mechanical properties of cartilage shape retention are accounted for by the development of areas of high internal stress upon mechanical deformation and the property of

shape memorization whereby shape recovery is possible after deformation.

In 1993, Emil Sobol et al. were the first to describe the use of lasers in altering cartilage shape [11]. Sobol hypothesized that local laser heating may lead to increased plasticity by relaxing the internal stresses, thereby leading to shape change with fluence rate profiles below the ablation threshold. Under ordinary conditions, mechanical resistance to sustained cartilage deformation is largely due to the intermolecular forces between water and proteoglycan models. Under moderate laser heating, Sobol hypothesized that there is a momentary relaxation in internal stress when water transitions from a state in which it is bound to proteoglycans to a liberated free state. If this bound-to-free phase transition of water can occur without damaging surrounding protein or carbohydrate molecules, then a stable modified cartilage configuration may be achieved.

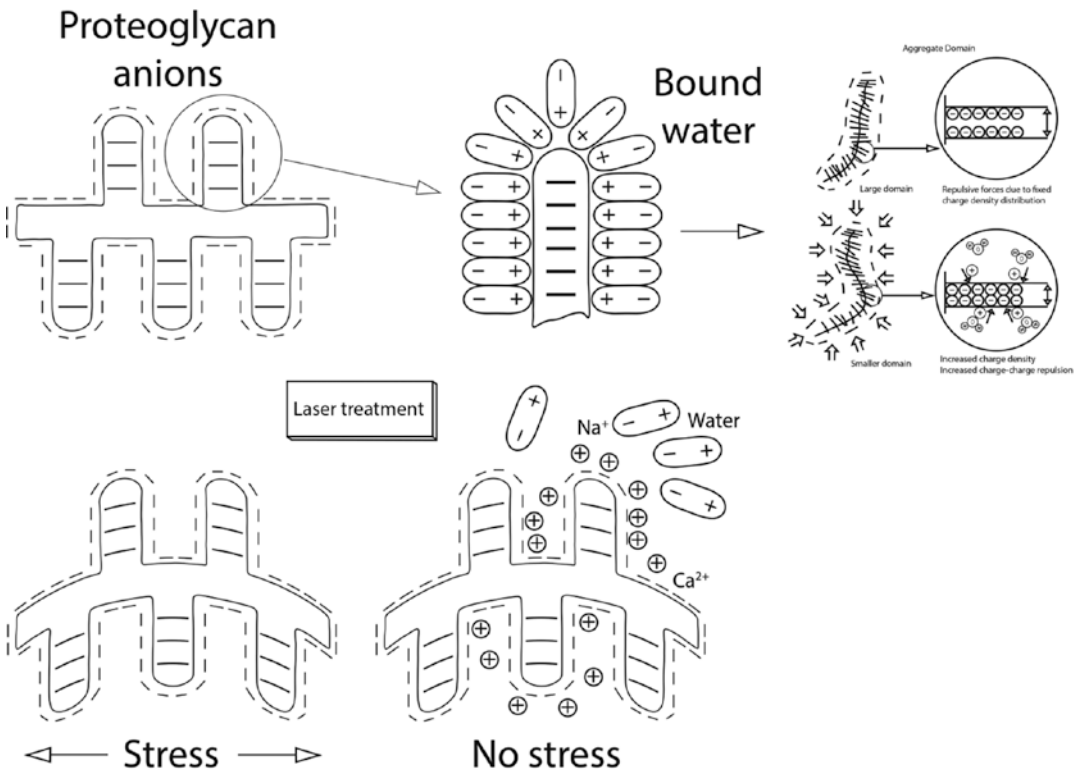


Fig. 13.1 Mechanisms of stress relaxation in cartilage (After Sobol et al. Laser Reshaping of Cartilage. Biotechnology and Genetic Engineering Reviews 2000 [10])

Sobol et al. demonstrated laser shape change on samples of cartilage from 0.2 to 1.5 mm in thickness using a CO₂ laser with 1–10 W in average power output. Cartilage samples were mechanically fixed in a new shape and exposed to either repetitively pulsed (pulse duration of 0.2 s, pulse repetition rate of 1 Hz) or continuous wave treatment regimens. Cartilage samples treated in this manner retained their shape for several months and could be implanted into animal models or kept in storage for later use, though banking of autologous cartilage is by no means common practice in North America.

13.2.2 Ex Vivo Cartilage Reshaping

After Sobol's initial studies on the use of lasers for reshaping cartilage, more detailed studies followed to characterize the effects of laser irradiation on tissue structure and viability and to attempt to identify optimal dosimetry. In subsequent studies, a holmium:YAG (Ho:YAG) laser (2.12- μm wavelength) was used to reshape a 1-mm-thick cartilage specimen without overheating or gross destruction of tissue near the surface [10]. Confocal microscopy and histology determined that thermal injury was deeper using Ho:YAG (up to more than 1800 μm) than with an Er:YAG laser (2.94 μm) as expected, suggesting that Ho:YAG lasers should be used judiciously with pulse energies as low as possible to reduce collateral tissue damage [12].

Atomic force microscopy images of the fine structure of cartilage following CO₂ laser irradiation showed the formation of micro-channels of 100–400 nm in cross section, lending some credence to a proposed mechanism for laser-induced stress relaxation of cartilage being based on short-time polymerization and subsequent reformation of proteoglycan units. These micro-channels may facilitate transport of traces of proteoglycan units possessing a length of ~300–400 nm and a width of ~80 nm. These results were also consistent with changes in light-scattering behavior in cartilage after laser-induced stress relaxation, whereby it is thought that the number of scattering centers first increases due to the short-time liberation of

proteoglycan units and then decreases after the new proteoglycan configuration has been formed. Furthermore, sodium carbonate crystals were observed, suggesting that prolonged laser heating of cartilage induces denaturation of proteoglycans and can lead to local mineralization of the cartilaginous matrix [13].

13.2.2.1 Dosimetry Studies

In 2000, Helidonis et al. performed histologic and morphological analysis on CO₂ laser-irradiated rabbit auricular cartilage to assess shape retention and viability [14]. Straight cartilage samples were removed from the ears of 21 rabbits, and the cartilage was reshaped using CO₂ laser at an output power of 3 W, a spot diameter of 2 mm, and exposure time of 0.5 s. Remodeled cartilage, along with control cartilage, was then implanted into the rabbits' backs and retrieved 6–12 months later, after which histology and morphological analyses revealed shape retention and viability of chondrocytes.

Subsequently, investigations were conducted to optimize parameters for cartilage reshaping and to define the therapeutic window within which cartilage is reshaped but not thermally damaged (Fig. 13.2). To this end, Wong et al. designed a computer-controlled instrument to evaluate the effect of laser dosimetry on shape change during laser-mediated cartilage reshap-

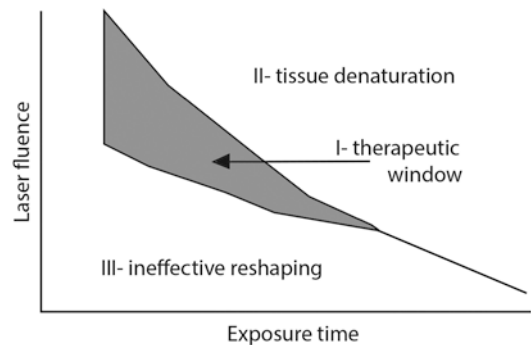


Fig. 13.2 Optimal therapeutic window, region of tissue denaturation, and ineffective reshaping as a function of exposure time and laser fluence (After Johansen, E. Determination of Optimum Laser Parameters for Cartilage Reshaping in Porcine Septum Using Nd:YAG Laser ($\lambda = 1.32 \mu\text{m}$) SPIE, 2001 [15])

ing using an Nd:YAG laser at a wavelength of 1.32 μm [15]. Real-time measurements of tissue optical properties and surface temperatures were obtained, and to determine optimal reshaping, the radius of curvature of the specimen was compared to that of the reshaping jig. Optimal reshaping was observed at 6 W with an irradiation time of 16 s or alternatively at 10 W with an irradiation time of 8 s.

Subsequent investigations focused on characterizing the safety of LCR by determining shape change and tissue viability as a function of laser dosimetry [16]. Similarly, Dobrikov et al. used changes in backscattered He-Ne light intensity to characterize the temperature range in which stress relaxation occurs [17]. Wong et al. utilized the same Nd:YAG laser at 1.32 μm as in previous studies but with a spot diameter of 5.4 mm instead of 5 mm; exposure times of 4, 6, 8, 10, 12, and 16 s; and powers of 4, 6, and 8 W. Cartilage surface temperature measured using infrared thermography and a live/dead viability assay combined with fluorescent confocal microscopy was used to determine the amount of thermal damage generated in irradiated specimens. Confocal microscopy identified dead cells spanning the entire cross-sectional thickness of cartilage specimen within the laser spot at laser power density and exposure times above 4 W and 6 s, with damage proportional to increases in time and irradiance. These results suggested that thermal tissue damage is concurrent with shape change and that significant cell death occurs at laser dosimetry parameters necessary to produce clinically relevant shape changes.

13.2.3 Cartilage Properties

Mow and Lai proposed a triphasic model of articular cartilage as an extension of their earlier biphasic theory [2, 3, 18]. The triphasic model consists of the following three phases: (1) an intrinsically incompressible porous permeable charged solid phase, (2) an intrinsically incompressible interstitial fluid phase, and (3) an ion phase with two monovalent ions (anion and cat-

ion). In this theory, the motive forces for water and ions are described by the gradient of chemical or electrochemical potentials. These driving forces are balanced by the frictional forces between the phases as one phase flows through the other. Stress and strain in cartilage is determined by a balance of tissue elastic properties, fluid flow or shift, and electrostatic charge. This model was later extended to incorporate multiple polyvalent ions by Gu et al. [19]

13.2.3.1 Optical Properties of Cartilage

In order to optimize laser cartilage reshaping (LACR), it was important to determine the optical properties of cartilage to facilitate computational modeling. It is well established in the literature that different types of cartilage have different structures and compositions. Sobol's group in 1993 demonstrated that light scattering may identify a phase transformation in cartilage after laser irradiation [20]. Bagratashvili et al. demonstrated that human, pig, and bovine cartilages have similar transmission and reflection spectra, which opened the door for the development of animal models for in vivo studies [21]. Wong et al. through a series of studies that measured integrated backscattered light intensity of He:Ne laser light ($\lambda = 632.8 \text{ nm}$) during laser irradiation by Nd:YAG laser ($\lambda = 1.32 \mu\text{m}$) observed an increase, plateau, and then decrease in diffuse reflectance during heating [22–24].

The above developments allowed for later studies by Youn et al. to further characterize optical and thermal properties of nasal septal cartilage using double integrating sphere experiments and thermocouple techniques [25]. Wong et al. demonstrated in 2001 that the tissue optical, mechanical, and biologic properties of septal cartilage varied spatially within each individual sample, as well as between animals within the same species [26]. These measurements would establish baseline values for tissue metabolism, cell density, and the basic biomechanical behavior of porcine and rabbit septal cartilage.

13.2.3.2 Thermal and Mechanical Properties of Cartilage

Stress Relaxation

From a materials science point of view, cartilage may be thought of as a charged polymer hydrogel, with a triphasic structure formed by the interplay of viscoelastic, hydrodynamic, and electrostatic forces. Early hypotheses by Sobol et al. on the mechanism of stress relaxation that occurs upon heating cartilage proposed that this phenomenon relied on a phase transformation dominated by the movement of the water through the matrix [27]. The underlying principle of this hypothesis is that water exists in two forms to form the structure of cartilage: bound, or non-exchangeable, and free, or exchangeable. Upon heating and deformation, a phase change between the two states of water within cartilage allows for stress relaxation to occur within the areas of highest stress, thereby allowing for shape change. The first of many studies to explore this hypothesis examined the thermodynamic characteristics of this “bound-to-free” phase transformation of water [28].

An important observation was made by Sobol et al. in 1997, where it was noted that light scattering increases with stress relaxation and at a temperature exceeding 70 °C [29]. Changes in light scattering were thought to represent the bound-to-free water phase transition, beginning with the formation of nucleus centers or local regions of anomalous refractive index created when water bound to large proteoglycan molecules becomes liberated. When examining the mechanical properties of cartilage following this phase transition, it was observed that stress indeed decreases with some time delay after tissue temperature reaches 70 °C, which was initially hypothesized to represent the internal friction coefficient of cartilage. These observations were used to develop theoretical models which incorporated thermal and mass transfer in a tissue to study the effect of laser irradiation, water evaporation from the surface, and the temperature dependence of the diffusion coefficient [30]. From this model, it was shown that surface temperature reaches a plateau quicker than the maximal temperature, laser-induced mass transfer in cartilage is hetero-

geneous along the depth, and depth of the denatured area depends on laser fluence, wavelength, exposure time, and thickness of cartilage.

Wong et al. investigated the pattern of backscattered light intensity and internal stress and found that both tend to increase, plateau, and then decrease in similar ways during laser irradiation [31]. The plateau region occurred when the cartilage surface temperature approached 65 °C. These observations clarified the potential of using backscattered light intensity to control the process of laser-assisted cartilage reshaping, which would allow for greater precision of heating, and minimize nonspecific thermal injury due to uncontrolled heating. Bagratashvili et al. examined the phase change through multiple modalities including optical coherence tomography [32]. They describe a bleaching effect similar to the increase in backscattered light described by earlier studies. This bleaching effect was due to structural alterations in irradiated cartilage caused by the removal of water; since water and cartilage matrix have different refractive indices, removal of water leads to increases in scattering signal.

Temperature Dependence of LCR

Although early reports show this transition to occur above 70 °C, later studies have described a range of critical temperatures T_c from 60 °C to 70 °C [31, 33]. To refine this range, Wong et al. studied temperature-dependent changes in thermal properties using modulated differential scanning calorimetry (MDSC), a very precise technique to measure temperature and heat flow associated with transitions in materials as a function of temperature and time [34]. It was observed that slow heating results in a lower critical transition temperature of around 55 °C, in contrast to the rapid heating associated with laser irradiation, with a critical transition temperature of around 65 °C. At around 70 °C, it was noted that heat flow into the specimen reaches a maximum and subsequently decreases, which is in agreement with previous results regarding temperature-dependent changes in optical and mechanical properties of cartilage. Further studies by Sobol et al. demonstrated that light scat-

tering may be useful for measuring denaturation thresholds and kinetics for biological tissues, with denaturation thresholds showing an inverse correlation with the absorption spectrum of the tissue [35].

Mechanical Properties

The elastic modulus describes the intrinsic stress-strain relationships in a material independent of geometry and is the best characterization of the mechanical behavior of cartilage. Investigations into the elastic modulus of cartilage samples contributed to the understanding of shape change in cartilage during laser irradiation and the optimization of this process. Gaon et al. determined the elastic moduli of porcine cartilage before and after Nd:YAG laser irradiation ($\lambda = 1.32 \mu\text{m}$, 21.22 W/cm^2) and found the elastic moduli to be much lower following irradiation [36]. This result confirms that cartilage becomes more flexible after undergoing stress relaxation due to photothermal heating. Gaon et al. also examined the changes in elastic moduli after total thermal denaturation of cartilage samples, which also resulted in a lower elastic modulus. However, the mechanical changes in elastic modulus after laser irradiation were reversible, whereas those following total thermal denaturation were not. Chao et al. conducted similar investigations on the elastic modulus of rabbit nasal septal cartilage and confirmed that this pattern of reversible decreases in elastic modulus is seen in the porcine model and is also seen in the rabbit model [37].

Thermal Properties

It has been hypothesized that cartilage reshaping occurs due to a heat-induced transition that leads to the rearrangement of molecular bonds in the cartilage matrix macromolecules. Chae et al. studied the thermomechanical behavior of cartilage using dynamic mechanical analysis (DMA) and time-temperature superposition (TTS)—techniques used in the rheological sciences to characterize viscoelastic material properties, such as storage and loss modulus, and damping properties [38]. They identified a temperature transition range between $50 \text{ }^\circ\text{C}$ and $67 \text{ }^\circ\text{C}$ —consistent with previous results. By using TTS, Chae et al. were

able to estimate the activation energy associated with the mechanical relaxation of cartilage as approximately 148 kJ/mole . This estimated activation energy for stress relaxation exceeds that of the evaporation of free water ($41\text{--}44 \text{ kJ/mole}$), as well as the activation energy of water diffusion (30.6 kJ/mole). Additionally, it was found that a relatively larger activation energy was required for relatively lower concentration of water. This may be due to an increased amount of energy needed to facilitate water movement through the dense ECM and liberate bound water from the proteoglycan side groups.

In order to estimate the thermal influence on the physical shape of a cartilage sample, Wright et al. rapidly immersed porcine nasal septal cartilage in saline water baths and measured resulting bend angles [39]. This was performed to emulate uniform or bulk volumetric heating of thin cartilage specimens held in deformation. The largest bend angle was seen at $74 \text{ }^\circ\text{C}$ with an immersion time of 320 s. In a following study, Wright et al. examined the dependence of cartilage shape change on both temperature and laser dosimetry using laser irradiation in addition to saline bath immersion [40]. From this investigation, the critical transition temperature region was determined by the sharp increase in bend angle at consecutive times of immersion at the same temperature ($59\text{--}68 \text{ }^\circ\text{C}$ and $62\text{--}68 \text{ }^\circ\text{C}$ for porcine and rabbit cartilage, respectively). As for laser irradiation, similar transition zones for dosimetry occurred below 20.4 W/cm^2 for both species.

In a later study by Chae et al., temperature modulate differential scanning calorimetry (TMDSC) is a technique that is used to differentiate between thermodynamic and kinetic components of heat flow [41]. From this analytic technique, two enthalpic events were identified in samples with low water loss, with the first event occurring between $50 \text{ }^\circ\text{C}$ and $52 \text{ }^\circ\text{C}$. When water loss exceeded about 35–40%, only one endothermic event was observed. Thus, the water content of the sample has a profound effect on the temperature range of phase transformation. Laser heating of cartilage creates a localized region of dehydration within cartilage samples within the area of light distribution. This variation in water

content could lead to changes in temperature thresholds for stress relaxation and thus phase transformation.

Modeling of Cartilage Reshaping

During laser irradiation of biological tissue, many important physical processes occur that determine temperature elevation and thermal damage rates. Of note are the propagation of light within a scattering media; transformation of laser light into photochemical, acoustic, or thermal energy; tissue-tissue and tissue-environment heat and mass transfer; and the occurrence of low-energy phase transformations. In order to optimize the reshaping process, it is essential to characterize the temperature-dependent stress relaxation and physical properties of cartilage, namely, elastic modulus, thermal diffusivity, and optical scattering. These processes have been used by Diaz et al. to create a finite element model (FEM) to predict the temperature distribution in a slab of porcine nasal cartilage during laser irradiation [42, 43]. These models can be used to make predictions of the onset, extent, and severity of thermal injury—information which may be used to develop dosimetry guidelines for medical applications of lasers.

In order to guide and optimize laser cartilage reshaping for clinical use in septal cartilage reshaping, Protsenko et al. used FEM to model the forces applied during cartilage straightening deformation before and after laser irradiation as a function of the number, pattern, and location of laser target sites [44]. From the FEM model, it was observed that straightening deformation produced a nonhomogeneous stress field with regions of tension and compression. With an increase in number of laser irradiation sites and delivered laser energy, it was noted that reaction force decreased. The model showed that in order to reduce reaction force by 95%, approximately 50% of thermal damage to septal cartilage would also occur.

13.2.3.3 Biophysical Properties and Cartilage Behavior

Cartilage is a charged, hydrated, protein-based polymer that is at risk for denaturation upon

heating. It is well known that laser heating may result in thermal decomposition of biopolymers as intermolecular bonds break as temperature rises. The safe practice of LCR necessitates investigation into thresholds of denaturation to minimize the risk of uncontrolled thermal injury. Tissue changes due to laser irradiation may be monitored by examining the number and size of light-scattering centers in the tissue, which has been discussed in previous sections for the application of monitoring the phase transformation of water in cartilage during laser-induced stress relaxation.

Sobol et al. used data on the time dependence of light scattering in tissue to estimate the approximate values of kinetic parameters for denaturation as a function of laser wavelength and radiant exposure [45]. An inverse correlation between denaturation thresholds and the absorption spectrum of the tissue was observed for many wavelengths. This was observed except at wavelengths near 3 and 6 μm , where denaturation threshold is instead governed by heating kinetics of tissue, as the initial absorption coefficient is very high. In a following study, Sobol et al. examined the alterations in the absorption of tissue water by laser heating with a short, single laser pulse with negligible movement and evaporation of water [46]. For temperatures less than 50 $^{\circ}\text{C}$, it was observed that the absorption coefficient for cartilage remained approximately constant. However, for temperatures above this critical threshold temperature, the absorption of coefficient decreases at a nearly constant rate. Therefore, the critical threshold temperature is the characteristic temperature for a change in the molecular structure of the tissue, and the changes observed are due to a decrease of intermolecular interaction energy, such as by the disaggregation of water molecules.

In another series of studies, Ignat'eva et al. investigated the thermal stability of collagen in cartilage and factors that may alter the degree of denaturation upon heating [47, 48]. Cartilage is composed primarily of type II collagen fibers embedded in a mesh-like network of proteoglycan fibers. In their 2004 results, Ignat'eva et al. generated the curve of endothermic melt-

ing of collagen and observed three peaks with maximums at 60, 65, and 70 °C. These peaks correspond to melting of three fractions of collagen: tropocollagen, fibril surface collagen, and fibrillary collagen, respectively. Analysis of thermal and thermomechanical behavior of the samples revealed that the initial melting point of the first fraction corresponded to the phase of softening of the preparations (40–50 °C), whereas the initial melting point of the third fraction (65 °C) corresponded to abrupt changes in sample shape. In their subsequent study, Ignat'eva et al. determined that hyaline cartilage, such as that of the nasal septum, is thermally stable and remains incompletely denatured up to 100 °C. However, partial destruction of glycosaminoglycans in hyaline cartilage leads to an increase in degree of denaturation of collagen II upon heating. Proteoglycan aggregates therefore may play a key role in creating topological hindrances for moving polypeptide chains, reducing the configurational entropy of collagen macromolecules during denaturation. Later, Hajjiioannou et al. determined the distinct role of the collagen network in cartilage shape and tensile strength pres-

ervation by enzymatically incubating cartilage strips and subsequently using laser irradiation for reshaping [49]. Collagen degradation was observed to be a substantial factor leading to the release of cartilage tensile stresses.

Polarization-sensitive optical coherence tomography (PS-OCT) has been used to characterize the polarization state of backscattered light as a function of optical path length in birefringent biological tissues. Birefringence in cartilage is due to asymmetrical collagen fibril structure, and changes in birefringence may signal disruption of cartilaginous structure due to laser irradiation. Youn et al. investigated the use of PS-OCT to measure thermodynamically induced changes of phase retardation in cartilage during LACR. It was observed that the retardation of light in the cartilage sample was changed due to laser irradiation, with two possible causes: dehydration and thermal denaturation (Fig. 13.3). The two conditions were then tested via either dehydration in glycerol or thermal denaturation in heated physiological saline. The results suggested that the observed retardation changes in cartilage were primarily due to dehydration.

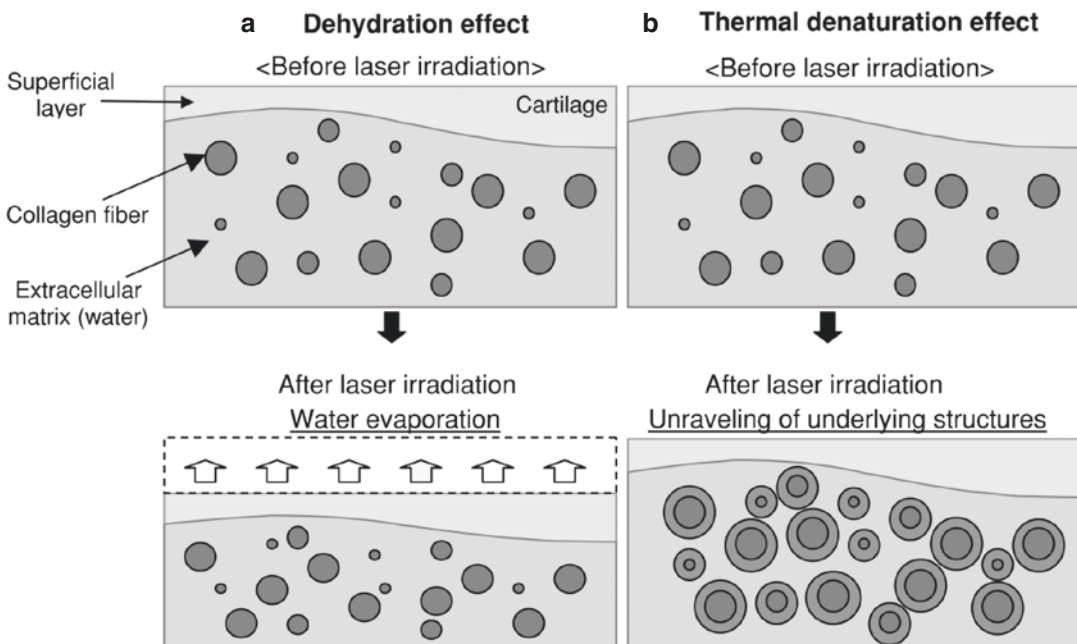


Fig. 13.3 Dehydration (a) and thermal denaturation effects (b) before and after laser irradiation (Youn et al. 2005 [48] © Institute of Physics and Engineering in Medicine. Reproduced by permission of IOP Publishing. All rights reserved)

Numerous methods have been used to evaluate phase transition during stress relaxation of cartilage samples undergoing LAR. Ultrasound monitoring can be used, as it has been demonstrated that the speed of the ultrasonic pulse is indicative of permanent stress relaxation [50]. By using a double integrating sphere system to measure diffuse transmittance, diffuse reflectance, and collimated transmittance of cartilage and polyacrylamide hydrogel samples as a function of temperature under 1560-nm laser irradiation, it was found that raising the temperature of cartilage samples to 80 °C caused the absorption coefficient to decrease by about 25% [51]. Other studies have shown that the effect of structural anisotropy of costal cartilage reveals itself in the increasing scattering of IR radiation passing crosswise the collagen orientation when tissue water content is decreased [52].

13.2.4 Control Systems in Laser Cartilage Reshaping

Since prolonged laser heating of cartilage leads to temperatures incompatible with chondrocyte survival, it is critical to develop a feedback system to control this process while still providing for adequate shape change. Wong et al. developed a feedback-controlled process utilizing an integrating sphere and silicon photodiode to measure backscattered light intensity. Additionally, a feedback-controlled cryogen spray was used to maintain surface temperatures below 50 °C [53]. Similar results were presented in a later study by Wong et al., where effective reshaping was also demonstrated [54]. Bagratashvili et al. have proposed a feedback mechanism integrating measurements of heat conductive or radiometric surface temperature of cartilage in addition to detecting backscattered light [55]. Burden et al. proposed using a thermopile to measure surface temperature, in addition to a silicon photoreceiver to detect backscattered light [56]. Sobol et al. have tested their feedback-controlled laser system on 380 patients with positive results obtained for 95% of patients with 2-year follow-up [57]. The following sections will discuss the

clinical use of feedback-controlled laser systems for cartilage reshaping.

13.3 Clinical Applications

13.3.1 In Vivo LCR

Cartilage reshaping has myriad clinical applications throughout head and neck surgery and has been an ongoing area of investigation for many decades. Classical approaches to altering the shape of cartilage in the head, neck, and upper airway have focused on manipulating the interlocking stresses and forces through partial thickness incisions or through sutures [58]. In the 1950s, Thomas showed that intravenous injections of the enzyme papain lead to reversible shape change in rabbit ears, an effect further potentiated by cortisone [59]. In the 1960s, De Palma then described that saline immersion of rabbit auricular cartilage would increase pliability and allow for shape change after at least 8 days of autotransplantation to the anterior abdominal wall [60]. Around that time, Rubin demonstrated the neutralization of interlocking stress forces through the use of morselization [61].

Although the above techniques were able to produce a shape change, this effect was not long-lasting or was achieved through invasive maneuvers. Laser cartilage reshaping provides a solution to both of these problems. The refinement and optimization of laser cartilage reshaping necessary for clinical use would involve investigations into the viability of chondrocytes following laser irradiation and understanding of the effect of laser dosimetry on tissue thermal injury.

Following the many *in vitro* and *ex vivo* studies that clarified the material properties of cartilage and the effects of laser irradiation, early *in vivo* studies were performed by multiple groups. Shapshay et al. induced tracheal wall collapse in beagles and irradiated tracheal cartilage under deformation with 1.44- μm Nd:YAG laser at 2 W of power with a spot of 3 mm on the mucosal side of the cartilage surface along the line where internal stresses were expected to be maximum

[62]. After 6 weeks, endoscopic examination displayed corrected tracheal wall with adequate airway, and histopathologically the overlying mucosa was fully regenerated, and a number of viable chondrocytes with normal appearance were observed within the local cartilage.

Omelchenko et al. reported similar findings in an *in vivo* investigation of porcine auricular cartilage reshaping [63]. Shape change was produced through irradiation by Ho:YAG laser of 2.1 μm with an energy from 0.1 to 1.0 J, pulse duration of 300 μs , and repetition rate of 5 Hz. They describe a set of zones corresponding to changes in cartilage structure expanding radially from the irradiated areas (Fig. 13.4). In the central zones 1 and 2, the cartilage matrix is nearly completely destroyed, with few viable chondrocytes. In the more peripheral zone 3, the matrix is not destroyed, but cell dystrophy is observed, and most peripherally, in zone 4, the matrix and chondrocytes are unchanged. At 2–4 months following laser irradiation, treated cartilage was observed to maintain shape change.

In multiple later studies, dosimetry, shape change, and chondrocyte viability were examined *in vivo*. Lowe et al. examined porcine ears following exposure to Ho:YAG laser irradiation at 2.1 μm with a pulse energy of 2 J/cm² at 20 Hz with a spot diameter of 1.1 mm for 7 s [64]. For this set of parameters, shape change was retained

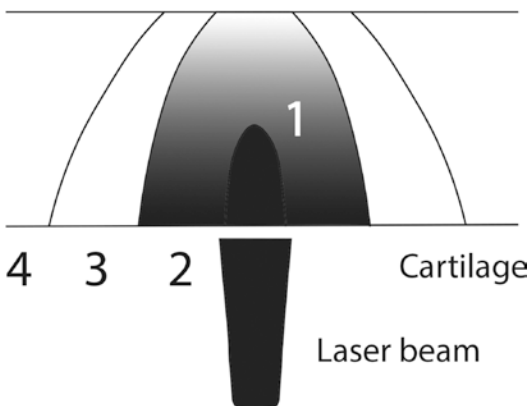


Fig. 13.4 The structural alteration zones induced by laser radiation in cartilage (*in vitro* experiment) (After Sviridov A. *In vivo* study and histological examination of laser reshaping of cartilage (1999, SPIE) [63])

for at least 14 days. Samples treated for less than 4 s returned to their original shape after 24 h, and those exposed for 9 s showed evidence of tissue necrosis. In all laser-irradiated areas, there was a loss of viable chondrocytes; however, in areas away from the center of irradiation, there was a marked proliferation of cartilage with a noticeable absence of any inflammation. Wong et al. examined an *in vivo* model of rabbit nasal septal cartilage reshaping using an Nd:YAG laser at 1.32 μm , 25 W/cm², and determined that shape change took place at the thermal range of 60–70 °C [65]. Creusy et al. examined multiple treatments in rabbit auricular cartilage using 1.54- μm Er:glass laser at 3 ms, 7 pulses, 12 J/cm², 2 Hz applied on 10 contiguous parallel rows along the ear, and examined biopsies from irradiated areas at 1, 3, and 6 weeks [66]. Shape change was observed in all treated ears. At 3 weeks, a chondroblastic proliferation was noted in areas of contracted cartilage, and at 6 weeks, the presence of new chondrocytes was observed.

13.3.1.1 Effects of LCR on Chondrocyte Viability

In general, chondrocytes are more sensitive to damage by laser irradiation than their surrounding ECM. The effect of laser irradiation on chondrocytes may be observed as either cytoplasmic focal vacuolation or nuclear condensation, representing reversible cell injury and cell death, respectively. Sviridov et al. showed in 1998 that there are conditions, such as laser fluence of 1.7 J/cm² and exposure time of 4 s, which allow for reshaping without nuclear condensation and only minor cell vacuolation. Lower values for these parameters produced less cell damage but were unfortunately not able to produce shape change [63].

The characterization of laser irradiation on cellular components of cartilage began with studies by Pullin, who investigated such effects from Ho:YAG irradiation in equine articular cartilage [67]. This study piggybacked off recent results showing potential applications for accelerating the healing process using laser irradiation and involved histological and biochemical assessments. Biochemical analyses included examina-

tion of GAG synthesis and cell proliferation at baseline and 24 weeks after irradiation between injured areas and an internal control. Their results demonstrated a clustering effect on chondrocytes at the exposure boundary, which may represent destructive changes or actual upregulation of chondrocyte metabolism. Additionally, they observed an inhibition of GAG synthesis in laser-treated perilesional tissue. However, no changes were noted on cell proliferation in irradiated areas, except in areas of lesional tissue, where increased proliferation was noted. This phenomenon may be caused by changes in the water diffusion kinetics in cartilage and the relaxation of the ECM.

Subsequent studies by Wong investigated proteoglycan synthesis in porcine nasal cartilage following Nd:YAG laser reshaping [68]. Cellular viability was evaluated by measuring the incorporation of $\text{Na}_2^{35}\text{SO}_4$ into proteoglycan macromolecules in whole-tissue culture. Wong et al. determined that average proteoglycan synthesis rates decreased with successive laser exposures but did not result in complete elimination of viable chondrocytes. The reduction in proteoglycan synthesis correlated with the time-temperature-dependent heating profile created during laser irradiation, which provided greater support to the need for careful monitoring of laser dosimetry to preserve chondrocyte viability.

In a later study, Wong et al. used flow cytometry to provide quantitative effects of laser irradiation on chondrocyte viability [69]. Porcine septal cartilages were irradiated with Nd:YAG laser with wavelength of 1.32 μm at 25 W/cm^2 , with exposure times of 6.7, 7.2, or 10 s. Samples were then examined immediately and at 5 days following laser exposure. Wong et al. determined that nearly 60% of chondrocytes were viable after one irradiation and that chondrocyte viability decreased to 31% and 16% after two and three exposures, respectively. A similar pattern was seen in samples 5 days following exposure, with the least amount of deterioration in untreated and singly irradiated samples.

Additional studies by Wong et al. demonstrated that thermal tissue damage is concurrent with shape change and that significant cell death

occurs at laser dosimetry necessary to produce clinically relevant shape changes both in rabbit septal cartilage [69] and in human septal cartilage [16].

13.3.1.2 Long-Term Viability

To determine long-term changes, Wong et al. examined the *in vivo* effect of laser dosimetry on rabbit septal cartilage integrity, viability, and mechanical behavior over 7 months [70]. In the first study, cartilage samples were treated with Nd:YAG laser across a broad dosimetry range (4–8 W and 6–16 s) and then examined 7 months later. In all laser-irradiated samples, variable tissue resorption and calcification were observed to correlate with increases in dosimetry. Elastic moduli of specimens were observed to be significantly different from controls, and viability assays demonstrated a total loss of viable chondrocytes within laser-irradiated zones. These results provided evidence against the presence of a laser dosimetry parameter space where the competing objectives of shape change and cell viability are both achievable and thereby underscore the importance of spatially selective heating.

13.3.2 LCR of the Airway

Deformities in the cartilages of the upper airway are a common problem encountered by the head and neck surgeon. Whether acquired or congenital, the standard treatment calls for serial endoscopic dilation, cartilage grafting, laser ablation, endotracheal stenting, tracheostomy, or segmental resection. Such invasive procedures bring significant potential for morbidity and mortality. Endoscopic laser reshaping of the trachea has been demonstrated in multiple studies and is a promising minimally invasive solution.

Early reports by Shapshay and Wang et al. on the *in vivo* use of Nd:YAG on dog tracheal cartilage demonstrated the remarkable effect on laser cartilage reshaping [71]. Six weeks post-operatively, all subjects had an adequate airway lined by healthy mucosa. Later studies by Wong et al. on *ex vivo* rabbit tracheal cartilage, selected to simulate the human neonate trachea,

by Er:glass laser determined that optimal parameters for shape change were at a wavelength of 1.54 μm and power of 1 W for a duration of 6–7 s [72]. At this setting, shape change was effected with minimal thermal injury. Subsequent studies by Wong et al. further investigated parameters for shape change, effect of temperature on the mechanical behavior of cartilage, and tissue viability, again in the rabbit model [73]. Shape change transition zones were observed between 62 °C and 66 °C in saline bath and above power densities of 350 J/cm². In line with previous results, a significant loss of viable chondrocytes within laser irradiation zones was observed.

Additional reports by Helidonis et al. show the potential of laser reshaping for the epiglottis, with applications for correcting laryngomalacia, obstructive sleep apnea resulting from epiglottal prolapse, and other congenital or acquired deformities of the epiglottis [74]. In a cadaveric model, they demonstrated the use of aCO₂ laser at 1560-nm wavelength and power density of 48 J/cm². Twenty to 30 pulses of 0.5 s or between 60 and 90 J were required to remodel the epiglottis.

13.3.3 LCR of Septal Cartilage

A patent nasal airway is critical for maintaining proper functioning of vocalization, humidification, filtration, heating of air, and adequate ventilation. Nasal airway obstruction can lead to subjective complaints while awake, as well as impairment while asleep, which potentially may lead to further complications such as reduced mentation, arrhythmia, and cor pulmonale.

Airflow through the upper airway can be approximated by Poiseuille's law, which states that flow is proportional to the fourth power of the radius of the tube. Therefore, even with small changes in airway radius, there may be a relatively large decrease in flow. Clinically, this reduction in flow may be observed at many levels of the upper aerodigestive tract. Nasal septum deviations are a common cause of airway obstruction, and until now, the standard of care for significant septal deviations has been through surgical correction.

The classical Indian textbook *Sushruta Samhita*, dating to around 600 B.C., was the first recorded description of nasal reconstruction [75]. Around this time, nasal fractures and gross septal deformities were corrected by manual manipulation. In the seventeenth century, Taglioacozzi and Brancas made advances in changing the external shape of the nose. Further advances were made in the eighteenth and nineteenth century including Freer and Killian's development of submucous resection of the nasal septum [76]. Contemporary septal surgery has evolved from Cottle, Loring, and Fisher's intranasal maxillary-premaxillary approach [77]. However, despite such advances, surgical correction of nasal septal deformities still requires most frequently general anesthesia and the potential for significant morbidity.

The development of laser cartilage reshaping brings the potential for a nearly bloodless procedure to achieve functional improvements in nasal airflow. The underlying principles of laser reshaping (discussed in greater detail at the beginning of this chapter) can be summarized in the steps of (1) mechanical deformation of tissue into desired shape and (2) laser irradiation of areas of highest internal stress, which results in (3) stress relaxation and stable shape change.

Historically, the use of laser-assisted cartilage reshaping was first utilized for septoplasty. Laser-assisted cartilage reshaping may be applied to native septal cartilage or, in cases where this is not possible, to autologous costal cartilage samples. Although costal cartilage is among the most suitable natural materials for transplantation, its natural semicircular curvature presents a challenge for obtaining a proper and stable shape. Optimal laser parameters have been extensively investigated and, in general, depend on multiple factors including thickness of tissue, its chemical composition, and structure.

13.3.3.1 Clinical Results of Laser Reshaping of Nasal Septal Cartilage

Advances in the clinical use of laser reshaping have been made by multiple groups within the past couple of decades. Starting in 2000, Sobol's group treated 40 patients with a holmium laser

and followed the effects of reshaping throughout the course of 12 months [78]. Even from this initial study, the results have been very promising. Twenty-three patients showed excellent long-term reshaping effects, 12 patients acceptably good results, and five patients with only marginal reshaping effects achieved. Thirty-five of the 40 patients reported a marked improvement in breathing, and no patient enrolled in the study displayed any visible undesirable side effects. In 2002, Ovchinnikov et al. followed 110 patients treated with Ho:YAG laser for an average of 18 months. Eighty-four patients were observed to display stable improvement in septal shape change and noted disappearance of any attendant symptoms [79]. Later in 2008, Bourolias et al. treated 64 patients using an Er:glass laser and followed for 6 months while recording average NOSE scores and flow and resistance measurements. In all of these metrics, they noted significant improvement without any intraoperative pain or postoperative complications [80].

In 2010, Leclere et al. followed 12 patients undergoing laser reshaping with an Er:glass laser with integrated cooling (Fig. 13.5) for the duration of 3 months. They were careful to do preoperative examinations including nasomanometry and nasal endoscopy to exclude inferior turbinate or adenoid hypertrophy. NOSE score was calculated at 1 week, 1 month, and 3 months post-procedure, and rhinomanometry was performed at 3 months.

They noted improvements in mean NOSE scores and improvements to air inflow resistance. Adequate septal reshaping was observed in seven adults, and in five adults incomplete septal reshaping was observed. Of the cases where the results were inadequate, anatomical variations such as a thick or a longer septum were hypothesized to be the causal factors. They also noted that inadequate local anesthesia prevented the completion of the procedure in two patients. However, following retreatment, all patients were able to achieve suitable reshaping [81].

These studies show that laser septal cartilage reshaping has the potential to be a safer alternative to surgical septoplasty that offers the potential for nearly painless and much less morbidity than conventional techniques.

13.3.4 LCR of Auricular Cartilage

Deformities in the external ear are estimated to occur in roughly one in every 5000 births. Common malformations include lack of antihelical folds or increased conchal-mastoid angles and have traditionally necessitated surgical correction by means of otoplasty. The technical difficulty of otoplasty is quite high, and as it requires precise placement of stitches or creation of cartilage-splitting incisions that precisely balance forces to resist deformation, otoplasty is

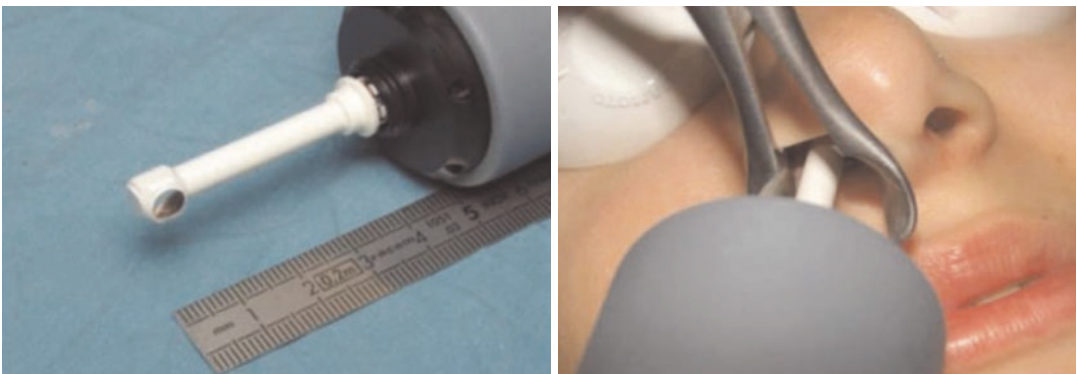


Fig. 13.5 Left image depicts handpiece allowing laser beam delivery at 90° and contact cooling (+5 °C) of the mucosa. Right image demonstrates treatment setup. Five stacked pulses (3 ms, 2 Hz, 50 J/cm² cumulative fluence) applied using 4-mm chilled handpiece at 5 °C temperature

on both sides of the septum (After Leclere et al. Laser-assisted septal cartilage reshaping (LASCR): A prospective study in 12 patients. *Lasers in Surgery and Medicine*, 42(8), 693–698. 2010 [81])

regarded as among the most difficult surgical procedures to master. With the advent of laser-assisted cartilage reshaping, the correction of auricular deformities may now be performed with much greater ease and simplicity.

In 2004, Mordon et al. at the French National Institute of Health and Medical Research (INSERM) proposed a method for reshaping protruding ears through 1.54- μm Er:glass laser irradiation in the rabbit model [66]. Rabbit ears were treated at fifteen spots applied on ten contiguous parallel rows (with parameters of 3 ms, 7 pulses, 12 J/cm², 2 Hz, 84/cm² cumulative fluence) while using a perforated cylindrical guide to determine ear curvature. Thermal damage was assessed via biopsies taken from irradiated areas at 1, 3, and 6 weeks. This initial study showed that with the parameters above, the skin was not visibly affected by laser irradiation, and every ear in the study was successfully reshaped. Furthermore, the authors noted chondroblastic proliferation around the area of contracted cartilage at 3 weeks and observed significant thickening of the cartilage layer along with the presence of new chondrocytes at 6 weeks. Perhaps most remarkable is that these results were achieved despite the substantial musculature within the rabbit ear.

In 2006, Mordon et al. conducted trials of LACR on human patients using the same 1.54- μm Er:glass laser [82]. In later reviews, it would

be determined that the 1.54- μm wavelength is ideal for cartilage reshaping of the ear, as the wavelength's penetration depth matches the thickness of the auricular cartilage, allowing for homogenous heat generation [83]. In this study, eight patients were treated with four undergoing LACR of both ears and four of only one ear. The entire concha and helix were irradiated on both sides with settings of 12 J/cm², seven pulses, 3 ms, 2 Hz, and 84/cm² cumulative fluence, applied with a 4-mm spot handpiece integrated in a cooling device. The integrated cooling, which resulted in about a 5 °C temperature drop, allowed for the procedure to be performed without the need for anesthesia. To produce shape change, a silicone elastomer mold was applied inside the helix and concha, and patients were asked to wear the resulting solid mold for 15 days using a bandage wrap. To assess for chondrocyte viability and epithelial damage, biopsies were taken immediately after LACR and subsequently at 1, 2, 3, and 4 weeks. The entire procedure could be performed in under 20 min per ear, was well tolerated, and was not associated with the development of hematomas or skin necrosis. Shape change was achieved in all patients, and all patients responded that the shape change met their expectations (Fig. 13.6). One patient had a mild recurrence of the upper antihelical fold; however, in all other cases, the reshaping was

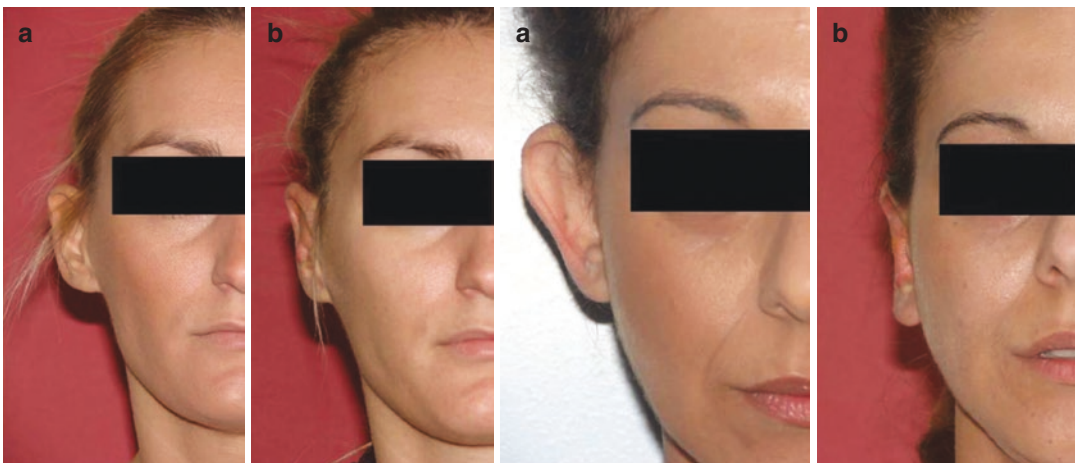


Fig. 13.6 Left and right series (a, b) show adult patient before (a) and 3 months after (b) LACR (After Leclere et al. Laser-assisted cartilage reshaping (LACR) for treat-

ing ear protrusions: A clinical study in 24 patients. *Aesthetic Plastic Surgery* 2010 [84])

found to be stable 6 months after LACR. Biopsy results showed discrete inflammatory reaction within the dermis at 1 week and a thickening of perichondrium and cartilage layers at 2 weeks, which was also observed at 3 and 4 weeks, along with viable chondrocytes.

A few years later, Leclere et al. presented their LACR results for treating protruding ears in 24 patients [84]. In order to determine optimal treatment parameters, the parameters used in this study were varied from those of previous studies by Mordon et al., with cumulative fluences ranging from 70 to 84 J/cm². In 21 of the patients, the 1.54- μ m Er:YAG laser was set to 12 J/cm² per pulse with seven stacked pulses (3 ms, 2 Hz, 84 J/cm² cumulative fluence) applied using a 4-mm spot handpiece with integrated cooling. For the remaining three adult patients, the laser was set at fluence of 10 J/cm² per pulse for a total cumulative fluence of 70 J/cm². All patients were given NSAIDs for 3 days after LACR and instructed to wear an elastomer mold at all times for 3 weeks and only at night for an additional 3 weeks. The authors noted six cases of contact dermatitis which they presume may be due to inappropriate mold design. In these cases, the patients stopped wearing the mold and thus did not achieve shape change. Otherwise, the authors note no cases of infections, hematomas, or skin necrosis. The remaining 18 patients achieved the expected outcome. At the lower fluence of 70 J/cm², the authors noted that incomplete reshaping was observed. The three patients treated at the lower fluence were re-treated at 3 months with 84 J/cm² fluence, and all achieved stable reshaping.

In 2010, Ragab described an open approach to the use of carbon dioxide laser, whereby the LACR is performed via evaporation of the perichondrium and laser incisions [85]. Sixteen patients were treated with application of the CO₂ laser directly onto the medial surface and posterior perichondrium of the auricular cartilages. A pair of parallel laser incisions was also created using a focused laser beam, reaching to a deeper thickness. Thirteen and 14 patients were pleased with the results at early and late assessment, respectively. McDowell's basic goals score was used as an objective measure of otoplasty

success, and the score was 4–6, with a mean of 5, with 6 as the total score. Hyperpigmentation, thermal injury, and other complications were not observed, and no revision surgery was needed even after 2.4 years of follow-up. The advantages of this open approach are the reduced reliance on external molds, which must be worn over an extended period, and a reduced recurrence rate.

Additional LACR treatment protocols have been studied using 1064-nm Nd:YAG lasers [86]. At this wavelength, there is a broader spectrum of absorption relative to the 1540-nm wavelength, which would allow for greater penetration depth. However, a few significant adverse effects were observed at 1064 nm, including skin burn and damage to auricular cartilage. The 2015 study by Leclere et al. was conducted on 14 patients who underwent 1065-nm LACR for protruding ears (repetition pulse emission of 1 Hz, 25-ms pulse length, 70 J/cm² fluence per pulse), with a beam diameter of 6 mm, using a handpiece with integrated cooling spray. It was noted with the above parameters that local anesthesia was necessary despite dynamic cryogen cooling. Despite the need for anesthesia and adverse effects, ten patients were pleased with the results, two patients satisfied, and one patient not satisfied. Overall, there were eight cases of localized skin burn and one case of dermatitis. Therefore, the authors conclude that the 1540-nm wavelength is superior due to the following: (1) the wavelength matches the cartilage thickness, (2) treatment is tolerated without anesthesia as long as contact cooling is available, and (3) it can achieve adequate reshaping.

The longest follow-up period investigated to date was conducted by Leclere et al. in 2011 [87]. In this study, Leclere et al. performed 32 LACR procedures in 17 patients and followed outcomes over a period of 30 months. A 1540-nm Er:glass laser set at 12 J/cm² with seven stacked pulses (3 ms, 2 Hz, 84 J/cm² cumulative fluence) applied using a 4-mm spot handpiece with integrative cooling was used to perform LACR. The authors note that treatment requires at least 50 (\times 7) pulses on each side of the auricular cartilage to be effective. The outcomes in this set of patients were similar to those seen in previous studies,

with no immediate complications seen. In the early postoperative period, two cases of contact dermatitis were noted due to inappropriate mold design. In five patients, a slight asymmetry was noticeable only by the surgeon after measuring cephalo-auricular distances. No other complications were noted, and overall satisfaction was 8.6/10 in the series.

13.3.4.1 Cryogen Spray Cooling in LCR

The development of a reliable cooling method was essential to bridge the gap between the bench and the bedside for LACR. As seen in the previous section, the success in applying LACR in the clinic depends on the ability to perform laser irradiation of the auricular cartilage without the need for anesthesia. This section will provide a concise overview of the development of cryogen spray cooling and explore its applications.

Early studies on the biomechanical properties of cartilage and material property changes due to laser irradiation determined that the critical temperature range of 60–70 °C marks the beginning of stress relaxation [27, 29, 34, 88]. Since protein denaturation occurs near 70 °C, this critical temperature range for cartilage reshaping must be precisely controlled, as extensive loss of cell viability may result in complete graft resorption, infection, and/or necrosis. Cryogen spray cooling (CSC) may be used to minimize excessive temperature elevations on the irradiated cartilage surfaces while allowing for homogenous axial temperature distributions within deeper portions of the irradiated cartilage. CSC involves the atomized delivery of a cryogen onto the skin surface 40–120 ms prior to laser irradiation. The evaporative cooling effect of the cryogen draws heat from the epidermis and allows for spatially selective thermal treatment of underlying cartilage.

In 2001, Karamzadeh et al. investigated the biophysical properties of cartilage and chondrocyte viability after LACR using CSC [89]. Chondrocyte viability was determined after 50 W/cm² Nd:YAG-mediated cartilage reshaping with and without CSC and correlated with dynamic measurements of tissue optical and thermal properties. This initial study found that after

2 s of laser exposure, specimens in both groups maintained shape change for up to 14 days. Chondrocyte viability was shown to correlate with the number of laser exposures. However, the relative viability in the cryogen controls was 99.58 ± 0.80%, suggesting that CSC along with the parameters used in this study do not contribute significantly to cell death.

In a later study by Cheng et al., optimization of laser and CSC parameters were determined on composite cartilage grafts (Fig. 13.7) from rabbit ears [90]. In this study, cryogen R134a (1,1,1,2-tetrafluoroethane) was applied to samples using a solenoid valve with a distance of 30 mm between the valve orifice to the sample. Cryogen was released at 50–70 mL/s spurts when surface temperatures on the outer portion of the bend exceeded 40 °C and ceased when thermocouple readings fell below 40 °C. Best results were obtained in specimens receiving 50 W with controlled CSC, with successful reshaping and minimal thermal damage.

The parameters for using CSC with LACR underwent further optimization with studies to determine therapy thresholds. Chlebicki et al. investigated optimal treatment parameters for laser output energy, CSC duration, and treatment cycles required to achieve shape change while limiting skin and cartilage injury [91]. Since this study attempted to identify therapy thresholds, aggressive parameters were used. Laser parameters resulting in acceptable skin injury to thick regions included the following parameters: 14 J/cm², a cryogen cooling spurt duration of 30–35 ms, and five to eight cycles. Unacceptable skin injury resulted from using 14 J/cm², a cryogen cooling spurt duration of 35 ms, and delivered in 10 cycles. When the CSC duration was reduced to 25 ms at 14 J/cm², unacceptable skin injury was also observed after six cycles. In thinner regions, parameters that resulted in unacceptable skin injury were the following: 13 J/cm² with CSC duration of 35 ms, delivered in six to seven cycles.

Since thicker tissues such as auricular cartilage may require higher laser power, and therefore increased cooling requirements, alternatives to conventional cryogens may provide a more

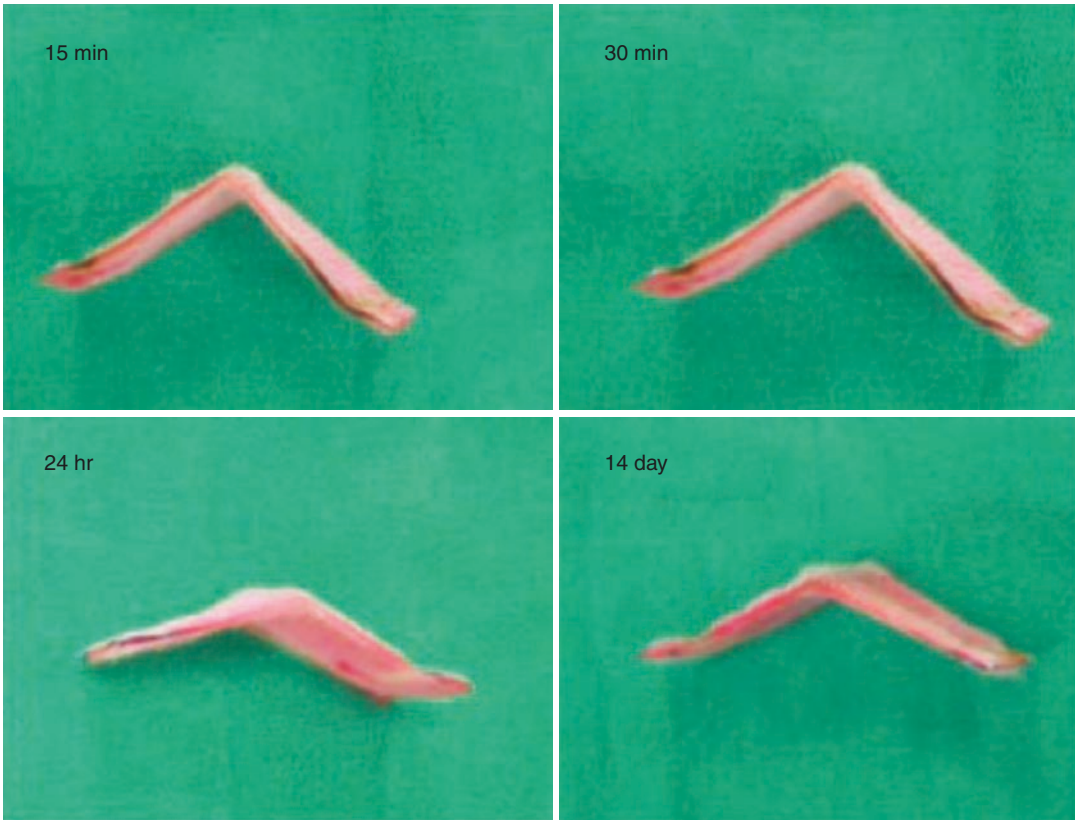


Fig. 13.7 A 50-W specimen shows most favorable deformation angle measuring 90° after initial elapsed time slot of 15 min. At the same wattage after 30 min post-illumination, the deformation angle remained at 90° . After 24 h, a small deformation angle of approximately 100° was measured. Deformation angle was maintained at about 100° and nonetheless produced a favorable angle, as

with other specimens of this group, that closely measured to that calculation throughout the remaining 14 days. (After Cheng et al. Minimizing Superficial Thermal Injury Using Bilateral Cryogen Spray Cooling During Laser Reshaping of Composite Cartilage Grafts. *Lasers in Surgery and Medicine*, 2008 [90])

optimal cooling effect. Wu et al. investigated the use of CO_2 spray cooling in ex vivo rabbit auricular cartilage [92]. CO_2 has the advantage of leaving no residue on skin, which reduces the risk of frostbite, has a lower environmental impact, and is economically cheaper than conventionally used cryogenes. Significant reshaping was achieved with all dosimetry tested, and with a $50\text{--}70^\circ\text{C}$ difference noted between controls and irradiated ears. The authors noted that increasing cooling pulse duration leads to progressively improved gross skin protection during irradiation.

The use of CSC in vivo has been investigated by Holden [93] and Kuan et al. [94] In

2009, Holden et al. showed that cartilage reshaping using 1450-nm diode laser combined with CSC may be used to safely perform LACR in the rabbit model. Parameters of 14 J/pulse with cryogen spray duration of 33 ms per cycle were used on experimental ears, with contralateral ears serving as internal controls. Adequate shape change was observed in all treated ears, and skin injury or post-procedural pain was not observed. In 2014, Kuan et al. used 1.45- μm wavelength diode laser along with CO_2 cooling in the in vivo rabbit model to show that shape change can be performed with minimal thermal cutaneous and cartilaginous injury (Fig. 13.8).



Fig. 13.8 Inversion of ears from same rabbit for bend angle measurement. This ear has been treated with laser and CO₂ (After Kuan et al. *In Vivo Laser Cartilage*

Reshaping with Carbon Dioxide Spray Cooling in a Rabbit Ear Model: A Pilot Study. *Lasers in Surgery and Medicine*, 2015 [94])

13.4 Conclusions

There has been a tremendous amount of work over the past few decades in optimizing the use of laser cartilage reshaping for clinical use. As we have examined laser cartilage reshaping from its development, through its many improvements and finally its clinical applications, we remain incredibly optimistic for what future developments may bring.

References

1. Wan LQ, Jiang J, Arnold DE, Guo XE, Lu HH, Mow VC. Calcium concentration effects on the mechanical and biochemical properties of chondrocyte-alginate constructs. *Cell Mol Bioeng.* 2009;1(1):93–102. <https://doi.org/10.1007/s12195-008-0014-x>.
2. Gu WY, Lai WM, Mow VC. A triphasic analysis of negative osmotic flows through charged hydrated soft tissues. *J Biomech.* 1997;30(1):71–8.
3. Lu XL, Wan LQ, Edward Guo X, Mow VC. A linearized formulation of triphasic mixture theory for articular cartilage, and its application to indentation analysis. *J Biomech.* 2010;43(4):673–9.
4. Lux Lu X, Miller C, Chen FH, Edward Guo X, Mow VC. The generalized triphasic correspondence principle for simultaneous determination of the mechanical properties and proteoglycan content of articular cartilage by indentation. *J Biomech.* 2007;40(11):2434–41.
5. McCluskey RT, Thomas L. The removal of cartilage matrix, in vivo, by papain; identification of crystalline papain protease as the cause of the phenomenon. *J Exp Med.* 1958;108(3):371–84.
6. Thomas L. The effects of papain, vitamin a, and cortisone on cartilage matrix in vivo. *Biophys J.* 1964;4(2):207–13.

7. Thomas L. Papain, vitamin A, lysosomes, and endotoxin. *Arch Intern Med.* 1962;110:782–6.
8. Thomas L, McCluskey RT, Potter JL, Weissmann G. Comparison of the effects of papain and vitamin A on cartilage I. The effects in Rabbits. *J Exp Med.* 1960;111(5):705–18.
9. Fell HB, Thomas L. Comparison of the effects of papain and vitamin A on cartilage. *J Exp Med.* 1960;111:719–44.
10. Sobol E, Bagratashvili V, Sviridov A, Omel'chenko A, Kitai M. Study of cartilage reshaping with holmium laser. *SPIE.* 1996;2623(95):544–7.
11. Helidonis E, Sobol E, Kavvalos G, Bizakis J, Christodoulou P, Velegrakis G, et al. Laser shaping of composite cartilage grafts. *Am J Otolaryngol.* 1993;14(6):410–2.
12. Frenzl M, Zuger BJ, Monin D, Weber HP, Schaffner T. Laser-induced cartilage damage: an ex-vivo model using confocal microscopy. *SPIE.* 1999;3601:115–20.
13. Sobol EN, Omelchenko AI, Mertig M, Pompe W. Scanning force microscopy of the fine structure of cartilage irradiated with a CO₂ laser. *Lasers Med Sci.* 2000;15:15–23.
14. Velegrakis GA, Papadakis CE, Volitakis ME, Nikolidakis AA, Naoumidi I, Prokopakis EP, Helidonis ES. In vitro ear cartilage shaping with carbon dioxide laser: an experimental study. *Ann Otol Rhinol Laryngol.* 2000;109(12):1162–6.
15. Johansen E, Burden M, Wong BJF. Determination of optimum laser parameters for cartilage reshaping in porcine septum using Nd:YAG Laser ($\lambda = 1.32 \mu\text{m}$). *Proc SPIE.* 2001;4257 <https://doi.org/10.1117/12.434706>.
16. Li C, Protsenko DE, Zemek A, Chae YS, Wong B. Analysis of Nd:YAG laser-mediated thermal damage in rabbit nasal septal cartilage. *Lasers Surg Med.* 2007;39(5):451–7. <https://doi.org/10.1002/lsm.20514>.
17. El Kharbotly A, El-Tayeb T, Mostafa Y, Hesham I. Diode laser (980 nm) cartilage reshaping. *SPIE.* 2011.
18. Lu XL, Mow VC. Biomechanics of articular cartilage and determination of material properties. *Med Sci Sports Exerc.* 2008;40(2):193–9. <https://doi.org/10.1249/mss.0b013e31815cb1fc>.
19. Gu WY, Lai WM, Mow VC. A mixture theory for charged-hydrated soft tissues containing multi-electrolytes: passive transport and swelling behaviors. *J Biomech Eng.* 1998;120:169–80.
20. Sobol EN. Phase transformations and ablation in laser-treated solids. New York: Wiley; 1995. p. 316–22.
21. Bagratashvi NV, Sviridov AP, Sobol EN, Kitai MS. Optical properties of nasal septum cartilage. *SPIE.* 1998;3254:398–406.
22. Wong BJF, Milner TE, Kim HK, Telenkov S, Chew C, Kuo T, Smithies DJ, Sobol EN, Nelson JS. Critical temperature transitions in laser mediated cartilage reshaping. *Proc SPIE.* 1998;3425:161–72.
23. Wong BJF, Milner TE, Anvari B, Sviridov A, Omel'chenko A, Bagratashvili V, Sobol EN, Nelson JS. Thermo-optical response of cartilage during feedback controlled laser-assisted reshaping. *Proc SPIE.* 1997;2970:380–91.
24. Wong BJF, Milner TE, Anvari B, Sviridov A, Omel'chenko A, Bagratashvili V, Sobol EN, Nelson JS. Measurement of radiometric surface temperature and integrated backscattered light intensity during feedback controlled laser-assisted cartilage reshaping. *Lasers Med Sci.* 1998;13:66–72.
25. Youn JI, Telenkov SA, Kim E, Bhavaraju NC, Wong BJ, Valvano JW, Milner TE. Optical and thermal properties of nasal septal cartilage. *Lasers Surg Med.* 2000;27(2):119–28. Retrieved from <http://www.ncbi.nlm.nih.gov/pubmed/10960818>
26. Wong BJF, Chao KKH, Kim HK, Chu BSEA, Gaon M, Sun C, et al. Laser mediated cartilage reshaping the porcine and lagomorph septal cartilages: models for tissue engineering and morphologic cartilage research. *Am J Rhinol.* 2001;15(2):109–16.
27. Sobol E, Sviridov A, Bagratashvili V, Omelchenko A. Stress relaxation and cartilage shaping under laser radiation. *SPIE.* 1996;2681:358–63.
28. Bagratashvili VN, et al. Thermal and diffusion processes in laser-induced stress relaxation and reshaping of cartilage. *J Biomech.* 1997;30:813–7.
29. Sobol EN, et al. Mechanism of laser-induced stress relaxation in cartilage. *SPIE.* 1997; <https://doi.org/10.1117/12.275495>.
30. Sobol EN, et al. Theoretical modeling of heating and structure alterations in cartilage under laser radiation with regard of water evaporation and diffusion dominance. *SPIE.* 1998; <https://doi.org/10.1117/12.308207>.
31. Wong BJF, Milner TE, Kim HH, Nelson JS, Sobol E. Stress relaxation of porcine septal cartilage during Nd:YAG (1.32 μm) laser irradiation: mechanical, optical, and thermal responses. *J Biomed Opt.* 1998;3:409–14.
32. Bagratashvili V, et al. Kinetics of water transfer and stress relaxation in cartilage heated with 1.56 μm fiber laser. *SPIE.* 2000;3914:102–7.
33. Wong BJF, et al. Critical temperature transitions in laser mediated cartilage reshaping. *SPIE.* 1998;3245:161–72.
34. Wong BJF, et al. Characterization of temperature-dependent biophysical properties during laser mediated cartilage reshaping. *IEEE J Sel Top Quantum Electron.* 1999;5:1095–102.
35. Sobol EN, et al. Effect of wavelength on threshold and kinetics of tissue denaturation under laser radiation. *SPIE.* 1999;3601:122–9.
36. Gaon MD, Ho KKH, Wong BJF. Measurement of the elastic modulus of porcine septal cartilage specimens following Nd: YAG laser treatment. *Lasers Med Sci.* 2003;18:148–53.
37. Chao KKH, Ho K-HK, Wong BJF. Measurement of the elastic modulus of rabbit nasal septal cartilage

- during Nd:YAG (1 1/4 1.32 Im) laser irradiation. *Lasers Surg Med.* 2003;32:377–83.
38. Chae Y, Aguilar G, Lavernia EJ, Wong BJB. Characterization of temperature dependent mechanical behavior of cartilage. *Lasers Surg Med.* 2003;32:271–8.
 39. Wright R, et al. Effect of bath water temperature and immersion time on bend angle during cartilage thermoforming. *SPIE.* 2003;4949:293–9.
 40. Wright R, Protsenko DE, Diaz S, Ho K, Wong B. Shape retention in porcine and rabbit nasal septal cartilage using saline bath immersion and Nd:YAG laser irradiation. *Lasers Surg Med.* 2005;37:201–9.
 41. Chae Y, Protsenko DE, Lavernia EJ, Wong BJB. Effect of water content on enthalpic relaxations in porcine septal cartilage. *J Therm Anal Calorim.* 2009;95:937–43.
 42. Diaz SH, Aguilar G, Lavernia EJ, Wong BJB. Modeling the thermal response of porcine cartilage to laser irradiation. *IEEE J Sel Top Quantum Electron.* 2001;7:944–51.
 43. Diaz SH, et al. Rate process analysis of thermal damage. *Phys Med Biol.* 2003;48:19–29.
 44. Protsenko DE, Wong BJB. Laser-assisted straightening of deformed cartilage: numerical model. *Lasers Surg Med.* 2007;39:245–55.
 45. Sobol E, Sviridov A, Kitai MS. Time-resolved, light scattering measurements of cartilage and cornea denaturation due to free electron laser radiation. *J Biomed Opt.* 2003;8(2):216–22.
 46. Sobol EN, Sviridov AP, Kitai MS, Edwards GS. Temperature alterations of infrared light absorption by cartilage and cornea under free-electron laser radiation. *Appl Opt.* 2003;42(13):2443–9. Retrieved from <http://www.ncbi.nlm.nih.gov/pubmed/12737481>
 47. Ignat'eva NY, Sobol EN, Averkiev SV, Lunin VV, Grokhovskaya TE, Bagratashvili VN, Yantsen ES. Thermal stability of collagen II in cartilage. *Dokl Biochem Biophys.* 2004;395(1–6):96–8. <https://doi.org/10.1023/B:DOBI.0000025555.66340.27>.
 48. Youn J-I, Vargas G, Wong BJB, Milner TE. Depth-resolved phase retardation measurements for laser-assisted non-ablative cartilage reshaping. *Phys Med Biol.* 2005;50(9):1937–50. <https://doi.org/10.1088/0031-9155/50/9/001>.
 49. Hajioannou JK, Nikolidakis A, Naumidi I, Helidonis E, Tzanakakis G, Velegrakis GA. In vitro enzymatic treatment and carbon dioxide laser beam irradiation of morphologic cartilage specimens. *Arch Otolaryngol Head Neck Surg.* 2006;132:1363–70.
 50. Ignat'eva NY, Averkiev SV, Lunin VV, Grokhovskaya TE, Obrezkova MV. Effect of supramolecular organization of a cartilaginous tissue on thermal stability of collagen II. *Russ J Phys Chem.* 2006;80(8):1336–41. <https://doi.org/10.1134/S0036024406080292>.
 51. Sviridov AP, Kondyurin AV. Optical characteristics of cartilage at a wavelength of 1560 nm and their dynamic behavior under laser heating conditions. *J Biomed Opt.* 2010;15(5):055003.
 52. Soshnikova YM, Keselman MM, Baum OI, Shults EV, Obrezkova MV, Lunin VV, Sobol EN. Effect of anisotropy and drying of costal cartilage on its optical transmittance in laser reshaping of implants with 1, 2, and 3 mm in thickness. *Lasers Surg Med.* 2016;48(9):887–92. <https://doi.org/10.1002/lsm.22575>.
 53. Wong BJB, Mimer TE, Anvari B, Sviridov A. Thermo-optical response of cartilage during feedback controlled laser-assisted reshaping intrinsic tissue turgor termed the donnan osmotic pressure. *SPIE.* 1997;2970:13–5.
 54. Wong BJ, Milner TE, Harrington A, Ro J, Dao X, Sobol EN, Nelson JS. Feedback-controlled laser-mediated cartilage reshaping. *Arch Facial Plast Surg.* 1999;1(4):282–7. Retrieved from <http://www.ncbi.nlm.nih.gov/pubmed/11430436>
 55. Bagratashvili NV, Dmitriev AK, Omel AI, Sobol N. Acoustic control of laser shaping of cartilage. *SPIE.* 1999;3732:312–8.
 56. Burden M, Johansen E, Wong BJB. Design and construction of a precision cartilage reshaping device. *SPIE.* 2001.
 57. Sobol EN, Sviridov AP, Svistushkin VM, Vorobieva NN. Feedback controlled laser system for safe and efficient reshaping of nasal cartilage. *SPIE.* 2010.
 58. Gibson T, Davis WB. Distortion of autogenous grafts: Its cause and prevention. *Br J Plast Surg.* 1958;10:257–74.
 59. Thomas L. Reversible collapse of rabbits ears after intravenous papain and prevention of recovery by cortisone. *J Exp Med.* 1956;104:245–51.
 60. De Palma RG, De Palma MT, De Forest M. Experimental alteration of the shape of rabbit ear cartilage. *J Surg Res.* 1964;4:2–6.
 61. Rubin FF. Permanent change in shape of cartilage. *Arch Otolaryngol.* 1969;89:64–70.
 62. Wang Z, Pankratov MM, Perrault DF, Shapshay SM. Laser-assisted cartilage reshaping: in vitro and in vivo animal studies. *SPIE.* 1995.
 63. Sviridov A, Sobol E, Bagratashvili V, Omelchenko A. In vivo study and histological examination of laser reshaping of cartilage. *SPIE.* 1999.
 64. Jones N, Sviridov A, Sobol E, Omelchenko A, Lowe J. A prospective randomised study of laser reshaping of cartilage in vivo. *Lasers Med Sci.* 2001;16(4):284–90. Retrieved from <http://www.ncbi.nlm.nih.gov/pubmed/11702634>
 65. Chang JC, Diaz SH, Wong BJB. Preliminary investigations of laser mediated cartilage reshaping in the in vivo rabbit model. *SPIE.* 2002.
 66. Mordon S, Wang T, Fleurisse L, Creusy C. Laser cartilage reshaping in an in vivo rabbit model using a 1.54 μm Er:Glass laser. *Lasers Surg Med.* 2004;34(4):315–22. <https://doi.org/10.1002/lsm.20029>.
 67. Pullin JG, Collier MA, Das P, Smith RL, DeBault LE, Johnson LL, Walls RC. Effects of holmium: YAG laser energy on cartilage metabolism, healing, and biochemical properties of lesional and perile-

- sional tissue in a weight-bearing model. *Arthroscopy*. 1996;12(1):15–25. Retrieved from <http://www.ncbi.nlm.nih.gov/pubmed/8838724>
68. Wong BJ, Milner TE, Kim HK, Chao K, Sun CH, Sobol EN, Nelson JS. Proteoglycan synthesis in porcine nasal cartilage grafts following Nd:YAG ($\lambda = 1.32$ microns) laser-mediated reshaping. *Photochem Photobiol*. 2000;71(2):218–24. [https://doi.org/10.1562/0031-8655\(2000\)071](https://doi.org/10.1562/0031-8655(2000)071).
 69. Rasouli A, Sun CH, Basu R, Wong BJF. Quantitative assessment of chondrocyte viability after laser mediated reshaping: a novel application of flow cytometry. *Lasers Surg Med*. 2003;32(1):3–9. <https://doi.org/10.1002/lsm.10142>.
 70. Karam AM, Protsenko DE, Li C, Wright R, Liaw L-HL, Milner TE, Wong BJF. Long-term viability and mechanical behavior following laser cartilage reshaping. *Arch Facial Plast Surg*. 2006;8(2):105–16. <https://doi.org/10.1001/archfaci.8.2.105>.
 71. Wang Z, Perrault DF, Pankratov MM, Shapshay SM. Endoscopic laser-assisted reshaping of collapsed tracheal cartilage: a laboratory study. *Ann Otol Rhinol Laryngol*. 1996;105(3):176–81.
 72. Tsang W, Lam A, Protsenko DE, Wong BJF. Endoscopic laser reshaping of rabbit tracheal cartilage: preliminary investigations. *SPIE*. 2005;2150:345–54.
 73. Chae Y, Protsenko DE, Holden PK, Chlebicki C, Wong BJF. Thermoforming of tracheal cartilage: viability, shape change, and mechanical behavior. *Lasers Surg Med*. 2008;40(8):550–61. <https://doi.org/10.1177/0145721709355835>.
 74. Bourolias C, Hajjioannou J, Sobol E, Velegrakis G, Helidonis E. Epiglottis reshaping using CO₂ laser: a minimally invasive technique and its potent applications. *Head Face Med*. 2008;4:15. <https://doi.org/10.1186/1746-160X-4-15>.
 75. Donald PJ. Homographic cartilage in facial implantation. *Facial Plast Surg*. 1992;8(3):157–75. <https://doi.org/10.1055/s-2008-1064646>.
 76. Rhinology. The collected writings of Maurice H. Cottle, MD. American Rhinologic Society. Editorial Board. Pat A. Barelli, Walter E.E. Loch, Eugene B. Kern, Albert Steiner; 1987. p 35–37.
 77. Cottle NH, Loring RM, Fisher GC, Gaynon IE. The maxilla-premaxilla approach to extensive nasal septum surgery. *Arch Otolaryngol*. 1958;68:303–13.
 78. Sobol EN, Sviridov AP, Bagratashvili VN, Omelchenko AI, Ovchinnikov Y, Shekhter A, et al. Laser reshaping of nasal septum cartilage: clinical results for 40 patients. *SPIE*. 2000.
 79. Ovchinnikov Y, Sobol E, Svstushkin V, Shekhter A, Bagratashvili VN, Sviridov AP. Laser septochondrocorrection. *Arch Facial Plast Surg*. 2002;4:180–5.
 80. Bourolias C, Prokopakis E, Sobol E, Moschandreas J, Velegrakis GA, Helidonis E. Septal cartilage reshaping with the use of an Erbium doped glass fiber laser. Preliminary results. *Rhinology*. 2008;46(1):62–5.
 81. Leclère FM, Petropoulos I, Buys B, Mordon S. Laser assisted septal cartilage reshaping (LASCR): a prospective study in 12 patients. *Lasers Surg Med*. 2010;42(8):693–8. <https://doi.org/10.1002/lsm.20958>.
 82. Trelles MA, Mordon SR. Correction of ear malformations by laser-assisted cartilage reshaping (LACR). *Lasers Surg Med*. 2006;38:659–62.
 83. Leclère FM, Vogt PM, Casoli V, Vlachos S, Mordon S. Laser-assisted cartilage reshaping for protruding ears: a review of the clinical applications. *Laryngoscope*. 2015;125:2067–71.
 84. Leclère FMP, Petropoulos I, Mordon S. Laser-assisted cartilage reshaping (LACR) for treating ear protrusions: a clinical study in 24 patients. *Aesthet Plast Surg*. 2010;34:141–6.
 85. Ragab A. Carbon dioxide laser-assisted cartilage reshaping otoplasty for prominent ears. *Adv Cosmet Otoplasty Art Sci New Clin Tech*. 2010:249–65. https://doi.org/10.1007/978-3-642-35431-1_24.
 86. Leclère FM, et al. 1064-nm Nd: YAG laser-assisted cartilage reshaping for treating ear protrusions. *Laryngoscope*. 2015;125:2461–7.
 87. Leclère FM, Mordon SR, Trelles MA. Cartilage reshaping for protruding ears: a prospective long term follow-up of 32 procedures. *Lasers Surg Med*. 2011;43:875–80.
 88. Helidonis A, Sobol E, Velegrakis G, Bizakis J. Shaping of nasal septal cartilage with the carbon dioxide laser—a preliminary report of an experimental study. *Lasers Med Sci*. 1994:51–4.
 89. Karamzadeh AM, Rasouli A, Tanenbaum BS, Milner TE, Wong BJF. Laser-mediated cartilage reshaping with feedback-controlled cryogen spray cooling: biophysical properties and viability. *Lasers Surg Med*. 2001;28:1–10.
 90. Cheng CJ, et al. Minimizing superficial thermal injury using bilateral cryogen spray cooling during laser reshaping of composite cartilage grafts. *Lasers Surg Med*. 2008;40:477–82.
 91. Chlebicki C, Protsenko DE, Wong BJF. Preliminary investigations on therapy thresholds for laser dosimetry, cryogen spray cooling duration, and treatment cycles for laser cartilage reshaping in the New Zealand White Rabbit Auricle Cara. *Lasers Med Sci*. 2014;10:54–6.
 92. Wu EC, et al. Ex vivo investigations of laser auricular cartilage reshaping with carbon dioxide spray cooling in a rabbit model. *Lasers Med Sci*. 2013;28:1475–82.
 93. Holden PK, Chlebicki C, Wong BJF. Minimally invasive ear reshaping with a 1450-nm diode laser using cryogen spray cooling in New Zealand White Rabbits. *Arch Facial Plast Surg*. 2009;48:1–6.
 94. Kuan E, et al. In vivo laser cartilage reshaping with carbon dioxide spray cooling in a rabbit ear model: a pilot study. *Lasers Surg Med*. 2015;19:161–9.